ACS APPLIED MATERIALS & INTERFACES

Research Article

www.acsami.org

Natural DNA-Modified Graphene/Pd Nanoparticles as Highly Active Catalyst for Formic Acid Electro-Oxidation and for the Suzuki Reaction

Konggang Qu, Li Wu, Jinsong Ren, and Xiaogang Qu*

Laboratory of Chemical Biology, Division of Biological Inorganic Chemistry, State Key Laboratory of Rare Earth Resource Utilization, Changchun Institute of Applied Chemistry, Graduate School of the Chinese Academy of Sciences, Chinese Academy of Sciences, Changchun, Jilin 130022, China

Supporting Information

ABSTRACT: Natural DNA has been considered as a building block for developing novel functional materials. It is abundant, renewable, and biodegradable and has a well-defined structure and conformation with many unique features, which are difficult to find in other polymers. Herein, calf thymus DNA modified graphene/Pd nanoparticle (DNA-G-Pd) hybrid materials are constructed for the first time using DNA as a mediator, and the prepared DNA-G-Pd hybrid shows high catalytic activity for fuel cell formic acid electro-oxidation and for organic Suzuki reaction. The main advantages of using DNA are not only because the aromatic nucleobases in DNA can interact through $\pi-\pi$ stacking with graphene basal surface but also because they can chelate Pd via dative bonding in such defined sites along the DNA lattice. Our results indicate that isolated, homogeneous, and ultrafine spherical Pd nanoparticles are densely in situ decorated on DNA-modified graphene surfaces with high stability and dispersibility. The prepared DNA-G-Pd hybrid has much greater activity and durability for formic acid electro-oxidation than the commercial Pd/C catalyst and polyvinylpyrrolidone-mediated graphene/Pd nanoparticle (PVP-G-Pd) hybrid used for direct formic acid fuel cells (DFAFCs). Besides, the DNA-G-Pd hybrid can also be an efficient and recyclable catalyst for the organic Suzuki reaction in aqueous solution under aerobic conditions without any preactivation. Since DNA can chelate various transition metal cations, this proof-of-concept protocol provides the possibility for the tailored design of other novel catalytic materials based on graphene with full exploitation of their properties.

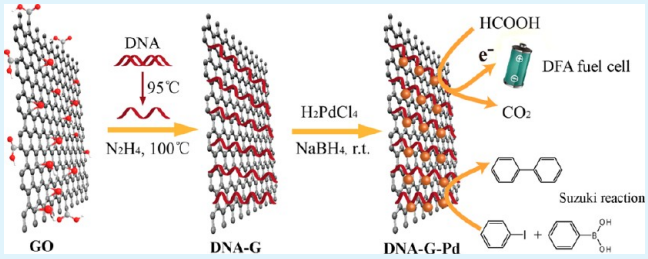

KEYWORDS: *Pd catalyst, graphene, natural DNA, formic acid electro-oxidation, suzuki reaction*

1. INTRODUCTION

Palladium has been emerging as a type of important catalyst in the development of industrial processes, in particular as an energy source and in fine chemical production. On the one hand, increasing energy demands have stimulated intense research on alternative energy conversion and storage systems with high efficiency, low cost, and environmental benignity.[1] Direct formic acid fuel cells (DFAFCs) have attracted great attention as a new generation of power sources with high operating power densities and low emissions.[2−7] Pd catalysts have become a hot topic of interest in the formic acid oxidation because of their lower cost, higher abundance, and greater resistance to CO as compared to Pt-based catalysts;[7] much effort has been devoted to developing simple and practical techniques to prepare Pd electrocatalysts with controllable micro/nanostructures and enhanced performance for the DFAFCs applications.[8−10] On the other hand, Pd functions as indispensable catalysts in petroleum cracking, hydrogenation, low-temperature reduction of automobile pollutants, and other organic reactions.[11] As an efficient catalyst in organic reactions, it can offer a favorable combination of activity and selectivity. These reactions are mostly carried out by homogeneous palladium organic complex systems; however, the high cost, low efficiency in separation, and subsequent recycling of homogeneous transition metal catalysts remains a scientific challenge and an aspect of economical relevance. One of the best ways to overcome this problem is the use of heterogeneous catalysis, i.e., solid-supported palladium catalysts, because of profound advantages of straightforward recovery and reuse of the catalyst from the reaction mixture by simple filtration, decantation, or magnetic altercations.[12−15] Therefore, the exploration of the highly active Pd catalysts has been one of the focuses of fuel cells and organic catalysis and has important practical significance in their industrial applications.

In recent years, graphene has aroused significant interests as a flat monolayer of carbon atoms tightly packed into a two-dimensional (2D) honeycomb lattice.[16,17] Since its discovery, graphene has shown many advantageous properties and can be

Received: July 19, 2012
Accepted: September 4, 2012
Published: September 4, 2012

Scheme 1. Schematic Illustration of the Procedure to Design Calf Thymus DNA-Modified Graphene/Pd Hybrid and the Catalysis Application in Direct Formic Acid (DFA) Fuel Cell and Suzuki Reaction

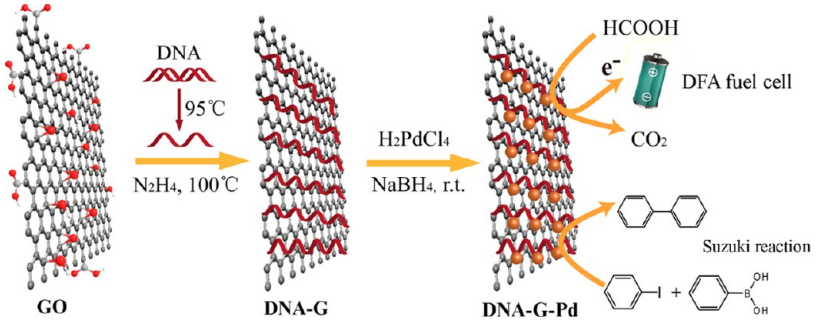

used in many nanoelectronic and optoelectronic devices and as a nanometer-scale building block for new nanomaterials.[18−23] Specially, its several excellent attributes, such as the huge theoretical specific surface area, excellent electronic conductivity, high chemical stability, and potential low manufacturing cost, make graphene the perfect catalyst support in fuel cells and heterogeneous catalysis.[24−30] Although a few examples involving the synthesis of graphene/Pd hybrids have been demonstrated to date,[27−29] some of the most critical issues yet to be improved are how to enhance the activity, durability, and recyclability of the graphene/Pd catalysts for fuel cells and heterogeneous catalysis and, accordingly, reduce their cost and minimize the environmental contamination.

To avoid the aggregation, the stabilizers are essential to pursue higher active catalysts which should have ultrafine sizes, outstanding dispersibility, and stability, such as surfactants,[31] polymers,[32] and dendrimers.[33] Natural DNA has emerged as an appealing biomacromolecule for electronic, optical, and biomaterials.[34] It is abundant, renewable, and biodegradable and possesses many unique properties difficult to find in other polymers. DNA's rich chemical functionality allows it to interact with a variety of nanomaterials of interest. The aromatic nucleobases in DNA can interact through $\pi-\pi$ stacking with graphene basal surface.[35] Transition metal cations, such as Ag,[36] Au,[37] Co,[38,39] Cu,[40] Pt,[41] and Pd,[42−44] can be chelated with the aromatic nucleobases in DNA via dative bonding. As a highly charged polyelectrolyte, the negatively charged phosphate groups on the DNA backbone can endow DNA-modified materials with high dispersibility in aqueous solutions. Therefore, these properties of natural DNA make it the ideal mediator to build graphene-based Pd catalyst.

Herein, we demonstrate utilization of natural calf thymus DNA in preparation of highly stable aqueous suspensions of graphene sheets. Then, palladium nanoparticles can be homogeneously in situ anchored onto the chemically modified graphene sheets by a facile route using DNA as the template (Scheme 1). The resulting calf thymus DNA-modified graphene/Pd (DNA-G-Pd) hybrid catalyst exhibits unexpected higher activity and superior durability in formic acid electrooxidation than commercial Pd/C catalyst and polyvinylpyrrolidone-mediated graphene/Pd nanoparticle (PVP-G-Pd) hybrid which can be attributed to the properties of DNA as the mediator that the common polymer PVP does not have. Moreover, in aqueous solution under aerobic conditions without any preactivation,[28] the prepared DNA-G-Pd is also verified to be an efficient, stable, and recyclable catalyst for the organic Suzuki reaction.

2. EXPERIMENTAL SECTION

Materials and Instrumentation. Graphite, hydrazine hydrate solution (85%), and polyvinylpyrrolidone (PVP) were purchased from Sinopharm Chemical Reagent Co. Ltd. (Shanghai, China). Calf thymus DNA (ctDNA) and Pd/C (containing 10 wt % Pd) was purchased from Sigma-Aldrich Chem Co.(USA), and ctDNA was purified as described earlier.[45] $PdCl_2$, H_2SO_4, HCOOH, and ethanol were purchased from the Shanghai Chemical Factory (Shanghai, China) and used as received without further purification. Sodium borohydride, sodium dodecyl sulfate (SDS), benzeneboronic acid, and iodobenzene were purchased from Alfa Aesar (USA). Nanopure water (18.2 MΩ; Millpore Co., USA) was used in all experiments.

UV−vis spectroscopy was carried out with a JASCO V-550 UV/vis spectrometer. Atomic-force microscopy (AFM) measurements were performed using a Nanoscope V multimode atomic force microscope (Veeco Instruments, USA). Scanning electron microscopic (SEM) images and energy-dispersive X-ray (EDX) analysis were recorded using a Hitachi S-4800 Instrument (Japan). Transmission electron microscopic (TEM) images were recorded using a FEI TECNAI G2 20 high-resolution transmission electron microscope operating at 200 kV. Thermogravimetry (TGA) was performed with a Pyres 1 TGA apparatus (Perkin-Elmer, MA) at a heating rate of 10 °C/min from 50 to 900 °C under a nitrogen atmosphere. XPS measurement was performed on an ESCALAB-MKII spectrometer (VG Co., United Kingdom) with Al Kα X-ray radiation as the X-ray source for excitation. Raman Spectra were obtained on a Labram HR Raman Spectrometer (Horiba-JY) with an excitation laser wavelength of 632 nm. XRD was measured on a Bruker-ANX D8 FOCUS diffractometer with Cu Kα radiation (λ = 0.15418 nm) operated at 40 kV and 40 mA. Gas chromatography was performed on a Shimadzu GC−17A system.

Synthesis of Graphite Oxide. Graphite oxide (GO) was synthesized from natural graphite powder by a modified Hummers method.[46] The detailed procedures were shown in the Supporting Information.

Preparation of ctDNA or PVP-Functionalized Graphene (DNA-G, PVP-G) Composites. The ctDNA was heated at 95 °C for 1−2 h to obtain single-stranded DNA. The GO dispersion (10 mL, 0.5 mg mL^{-1}) was mixed with single-stranded DNA (10 mL, 2 mg mL^{-1}) or 40 mg of PVP, and hydrazine was added (8 μL, 85 wt %; hydrazine/GO weight ratio = 7: 10); the mixture refluxed at 100 °C for 1 h. Then, the solution was centrifuged and washed several times with double-distilled water and dissolved in 10 mL of water to obtain DNA-G or PVP-G composites (0.5 mg/mL). As a control, chemically reduced graphene (CRG) is prepared by the similar methods, just without PVP or DNA as stabilizer during the reduction process.

Synthesis of Different Graphene-Based Pd Catalysts. The H_2PdCl_4 aqueous solution (0.5 M) was prepared by mixing 177.4 mg of $PdCl_2$, 1 mL of 2 M HCl, and 1 mL of H_2O. One hundred microliters of DNA-G or PVP-G or GO aqueous solution (0.5 mg/mL) and 5.6 μL of H_2PdCl_4 aqueous solution were added to the final 1 mL aqueous solution, and then, 20 μL of freshly prepared $NaBH_4$ solution (5 mg/200 μL H_2O) was added and stirred for only 1 min at room temperature. Then, the solution was centrifuged and washed

dx.doi.org/10.1021/am301376m | ACS Appl. Mater. Interfaces 2012, 4, 5001−5009

several times with double distilled water and dissolved in 0.5 mL of water to obtain DNA-G-Pd, PVP-G-Pd, or GO-Pd catalyst, respectively. GO-Pd catalyst was reduced by N_2H_4 to obtain rGO-Pd catalyst.

Electrocatalytic Experiment. All electrochemical measurements were carried out with the CHI 660b electrochemical workstation, using a three-electrode test cell. A conventional three-electrode system was used with a modified glassy carbon electrode (GCE, Φ = 3 mm, CHI) as the working electrode, a Pt wire as counter electrode, and an Ag/AgCl (saturated KCl) electrode (SCE) as reference electrode. The GCEs were polished successively with 1.0, 0.3, and 0.05 mm alumina (Buhler) and sonicated for 3 min before modification. For elelctrocatalysis, 20 μL of each graphene-based Pd catalyst solution or Pd/C dispersed in ethanol (containing 11.92 μg of Pd of equal mass) was dropped on the surface of the GC electrode and dried with an infrared lamp. All electrolytes were deaerated by bubbling N_2 for 30 min and protected with a nitrogen atmosphere during the entire experimental procedure. All experiments were carried out at a temperature of 25 °C.

Suzuki Reaction Catalyzed by Graphene-Based Pd Catalysts. Iodobenzene (20.4 mg, 1.0 mmol) was added to a stirred mixture of SDS (14.4 mg, 0.5 mmol), tripotassium phosphate (K_3PO_4, 39.9 mg), phenylboronic acid (14.6 mg, 1.2 mmol), and deionized water (H_2O) (2 mL), followed by each graphene-based Pd catalyst or Pd/C (1.1 mol %). The mixture was then stirred at 100 °C in an oil bath, and the extent of the reaction was monitored by TLC (thin-layer chromatography); the reaction mixture was then extracted with ethyl acetate (3 × 2 mL), the combined organic extract was dried over anhydrous sodium sulfate (Na_2SO_4), and the resulting mixture was analyzed by gas chromatography (GC). The catalysts were recovered by simple centrifugation and washed extensively with acetone and deionized water. The same procedure was conducted in other solvents (ethanol, 85% ethanol/15% water, and 50% ethanol/50% water).

3. RESULTS AND DISCUSSION

Preparation and Characterization of Graphene/Pd Hybrid Catalysts. In the process of designing new graphene/Pd hybrids, we use stabilizers to enhance the dispersibility of the reduced graphene and the growth of Pd nanoparticles (NPs) at the surface of graphene. We generated four different types of graphene/Pd hybrid catalysts: DNA-G-Pd, PVP-G-Pd, GO-Pd, and rGO-Pd catalysts to assess the influence of different stabilizers and the reduction extent of grapheme compared with the commercial Pd/C catalyst. The preparation of four different types of catalysts is described step by step in the Experimental Section.

The reduction of GO and the formation graphene/Pd hybrids can be monitored by UV−vis spectroscopy (Figure 1).[47,48] The UV−vis spectrum of GO contains a strong absorption band at 230 nm and a weak band around 300 nm, which correspond to C═C $\pi \rightarrow \pi^*$ and C═O n $\rightarrow \pi^*$ transitions, respectively. After the reduction, the absorption peaks of DNA-G and PVP-G composites redshift from 230 to 269 nm, suggesting that the electronic conjugation within graphene sheets is restored after the reaction. The color change of solution from brown to dark also indicates the reduction of GO. The disappearance of the absorption of H_2PdCl_4 at 425 nm indicated Pd^{2+} has been reduced to Pd NPs. The Pd loading level is very high up to approximately 85 wt %, which should be attributed to the huge specific surface area of graphene. At concentrations of 0.5 mg/mL, the resulting DNA-G, PVP-G, and the corresponding graphene-based Pd catalysts are very stable in aqueous solution, even for several months' storage without precipitate due to the highly soluble DNA and PVP as the stabilizers facilitating the dispersibility of the resulting hybrids. The GO-Pd catalysts can only keep stable for a few days, but the precipitate would be dispersed again after ultrasonication because of the presence of the oxide groups. The rGO-Pd catalyst exists as an agglomerate and has no any dispersibility even under ultrasonication.

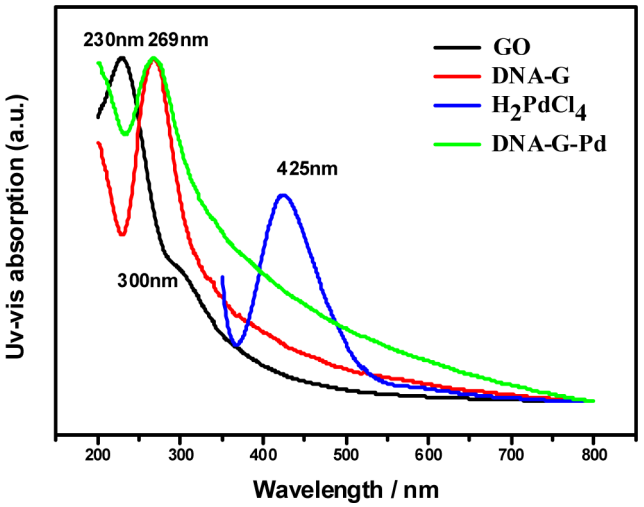

Figure 1. UV−vis absorption of GO (black), DNA-G (red), H_2PdCl_4 (blue), and DNA-G-Pd hybrid (green).

The morphologies of the four kinds of graphene/Pd hybrid catalysts were characterized using transmission electron microscopy (TEM) and tapping mode atomic force microscopy (AFM) studies (Figures 2, 3, and 4). TEM images show that GO and DNA-G and PVP-G composites are well-dispersed ultrathin flat sheets ranging from 200 nm to more than 1 μm in size and have occasional folds, crinkles, and rolled edges, indicating that both DNA and PVP can stabilize the reduced graphene ascribing to the $\pi-\pi$ interaction and hydrophobic interaction, respectively.[35,49] However, TEM images (Figure 2) of the four kinds of as-prepared graphene-based Pd catalysts show different morphologies. For DNA-G-Pd catalyst, isolated, homogeneous, and ultrafine spherical Pd NPs are densely assembled on the graphene surface with the mean size of about 4.8 nm (Figure 3). However, Pd NPs on the PVP-G composites with the mean size of about 5.2 nm exhibit small aggregations formed by several nanoparticles. The different morphologies of Pd NPs can be related to the difference between DNA and PVP. For calf thymus DNA, each nucleobase contains multiple nitrogen functional groups including exocyclic amino group and imino group, whereas the structural unit of PVP only has one tertiary amine, so calf thymus DNA has a much higher density of the nitrogen functional groups than PVP, which served as favorable nucleation and defined sites for Pd NP chelating via dating bonding to form stable and dispersed Pd NPs along the DNA lattice. For GO-Pd catalyst, large and different shaped Pd NPs are randomly distributed on the GO surface with an extremely wide size distribution of several tens of nanometers (mean size: 45.4 nm) because of the lack of stabilizers. The Pd NPs on the rGO-Pd show similar morphology with the GO-Pd catalyst (mean size: 42.1 nm), but the rGO-Pd exists as bulk agglomerations owing to the loss of functional groups and lack of stabilizers. The HRTEM images of Pd NPs show the spacing of the lattice fringes (0.225 nm) of Pd nanoparticles, which corresponds to the Pd (111) crystalline planes.[28] AFM images (Figure 4) indicate that the GO sheets are 1−1.2 nm in thickness, confirming the formation of fully single atomically thick GO layers. In contrast, the apparent height of the DNA-G

dx.doi.org/10.1021/am301376m | ACS Appl. Mater. Interfaces 2012, 4, 5001−5009

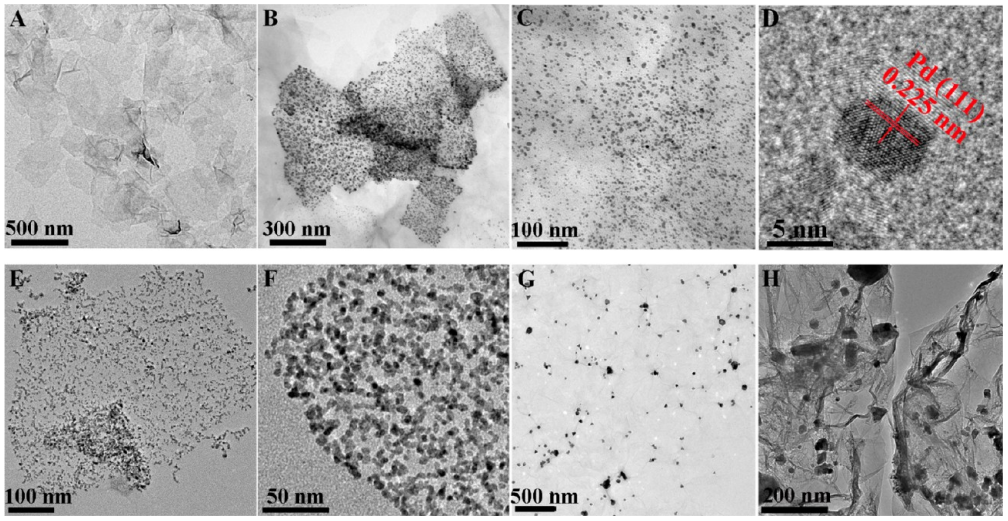

Figure 2. TEM images of (A) DNA-G and (B, C) DNA-G-Pd hybrid; (D) HRTEM images of DNA-G-Pd hybrid, (E, F) PVP-G-Pd, (G) GO-Pd, and (H) rGO-Pd.

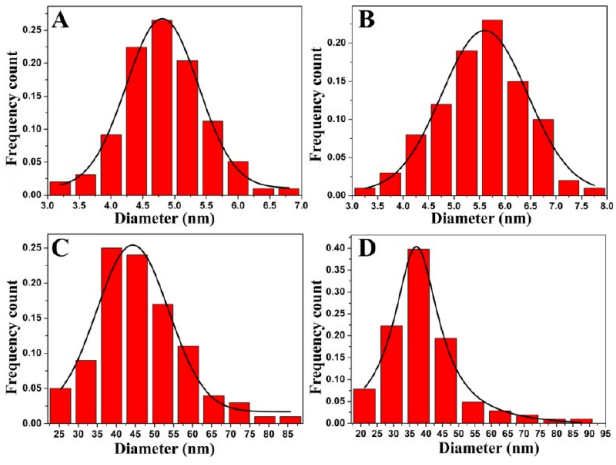

Figure 3. The corresponding particle size distribution histogram of Pd NPs on different hybrids: (A) DNA-G-Pd hybrid, (B) PVP-G-Pd hybrid, (C) GO-Pd hybrid, and (D) rGO-Pd hybrid (based on statistical analyses of more than 150 particles from TEM images).

and PVP-G sheets are about 2.4 and 2.6 nm, respectively, which correspond to the adsorption of single-stranded DNA and PVP molecules on both sides of the reduced graphene sheets.[35]

Typical images of DNA-G-Pd and PVP-G-Pd show that both of them have a rougher surface than the corresponding graphene sheets, indicating Pd NPs are facilely adsorbed on the surface of graphene nanosheets. The height of the Pd nanoparticles on graphene is in the range of 4−6 nm. However, PVP-G-Pd has more obvious aggregates than DNA-G-Pd, which is consistent with the results of TEM analysis.

Structural features of the prepared composite samples were studied by X-ray diffraction (XRD). As displayed in Figure 5, the XRD peak of GO was observed at 2θ = 10.4°, corresponding to an average interlayer spacing of ∼0.85 nm due to the presence of oxygen-containing functional groups attached on both sides of the graphene sheets. In contrast, after reduction, thin films prepared from DNA-G and PVP-G dispersions show low angle reflections at 2θ = 5.3° and 4.5° (Figure S1, Supporting Information), respectively, that correspond to an expanded interlayer spacing (d_{001}) of 1.7 and 1.9 nm due to the adsorption of single-stranded DNA and PVP chains, respectively. It also reveals that PVP-G has a slight larger interlayer spacing than DNA-G, which is consistent with the result from the AFM analysis. For the patterns of the four graphene/Pd hybrids including DNA-G-Pd, PVP-G-Pd, GO-Pd, and rGO-Pd, all of them have crystalline structure of Pd with peaks emerging at 39.8°, 46°, 67.8° and 81.6°,

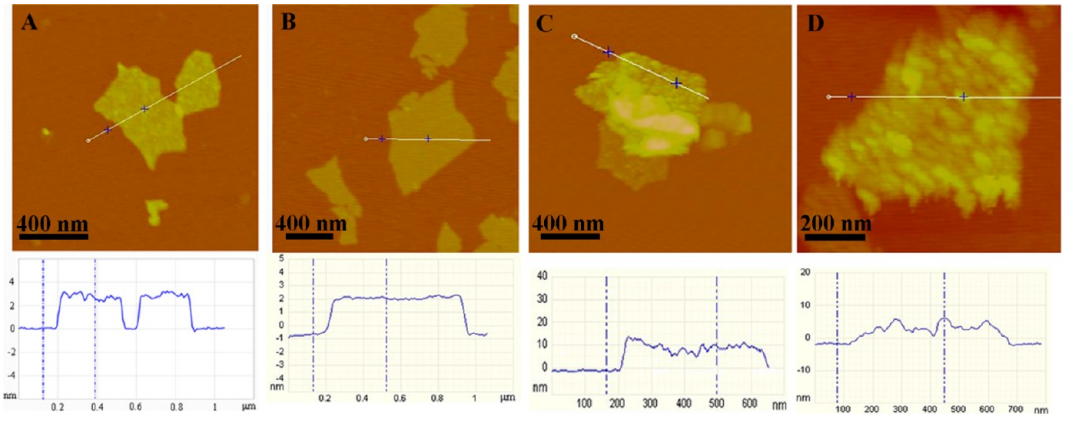

Figure 4. AFM images of (A) DNA-G, (B) PVP-G, (C) DNA-G-Pd, and (D) PVP-G-Pd hybrids.

dx.doi.org/10.1021/am301376m | ACS Appl. Mater. Interfaces 2012, 4, 5001−5009

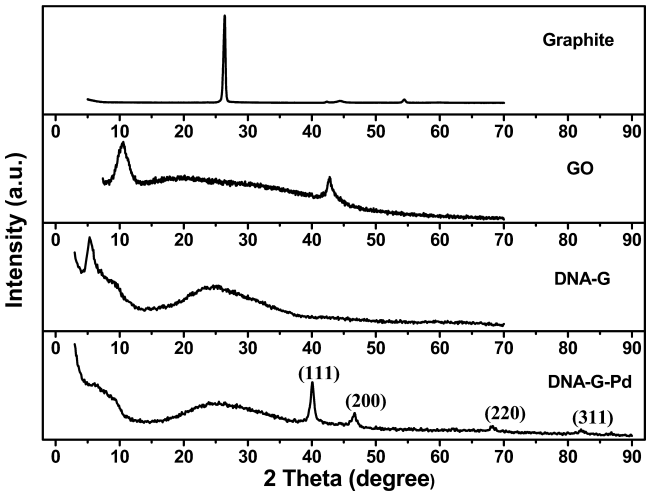

Figure 5. XRD patterns of graphite, GO, DNA-G hybrid, and DNA-G-Pd hybrid.

corresponding to the (1 1 1), (2 0 0), (2 2 0), and (3 1 1) planes of face-centered cubic structure of Pd, respectively, further confirming the formation of Pd nanoparticles from the precursor H_2PdCl_4.[9]

Raman spectra can reflect structural changes of graphene.[28,50] As shown in Figure 6, the spectrum of GO has two peaks at 1353 and 1597 cm^{-1} ascribed to the D and G bands of graphene, respectively. The D band corresponds to defects in the curved graphene sheet and staging disorder, while the G band is related to the vibration of sp^2-bonded carbon atoms in a 2D hexagonal lattice. Raman spectrum of DNA-G also contains both D and G bands (at 1327 and 1598 cm^{-1}, respectively), however, with an increased D/G intensity ratio (I_D/I_G = 1.02) compared to that in GO (0.96). It has been well documented that the average size of the sp^2 domains is the inverse of I_D/I_G.[51] On the basis of the empirical Tuinstra−Koening relation,[51] we found that the average size of the sp^2 domains was decreased from ~4.6 nm of GO to ~4.3 nm of DNA-G upon reduction. Meanwhile, the shift of D band from 1353 to 1327 cm^{-1} may be ascribed to the reduction of graphene oxide and the $\pi-\pi$ interactions between single-stranded DNA and the graphene basal plane. The value of I_D/I_G (1.09) for DNA-G-Pd is greater than that of DNA-G, which indicates the interactions occurred between Pd nanoparticles and DNA-G. Such an enhancement has also been observed in examples of GO[52] and carbon nanotubes[53] decorated with metal nanoparticles, indicating chemical interaction or bonding between the metal nanoparticles and graphene.

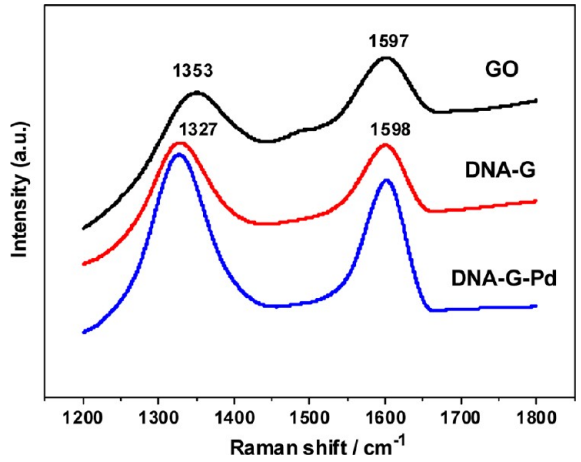

Figure 6. Raman spectra of GO (black), DNA-G (red), and DNA-G-Pd (blue).

The compositions of these catalysts were further analyzed by using thermogravimetric analysis (TGA), energy-dispersive X-ray spectroscopy (EDX), and X-ray photoelectron spectroscopy (XPS) techniques. As shown in Figure 7, the TGA results show that the DNA-G and PVP-G composites contain about 15 wt % DNA and 24 wt % PVP, respectively. The corresponding EDX results (Figure S2, Supporting Information) of DNA-G-Pd shows the peaks corresponding to C, O, N, P, and Pd elements, clearly confirming the existence of Pd NPs on the surface of DNA-G sheets. XPS is an efficient method to analyze chemical state information of elements, which provided quantitative information about the type and extent of surface functionalization present on the GO and DNA-G and DNA-G-Pd hybrid samples (Figure 8). As for the GO sheets, the C1s spectrum consists of four components: a strong peak at 284.6 eV corresponding to the C═C bond (43.4%), a weak peak at 285.5 eV corresponding to the C−O bond (4.4%), and two components at 286.7 and 288.3 eV attributable to the C−O−C bond (42.6%) and C═O bond (9.6%).[35] Analogous studies on samples of DNA-G showed a similar restoration of aromaticity and confirmed the presence of DNA on the graphene surface. Carbon species attributed to DNA molecules included C−N and N−C−N (45.6%, 286.3 eV), amide (N−C═O, 5.7%, 287.8 eV), and urea (N−C(═O)−N, 6.2%, 288.3 eV)

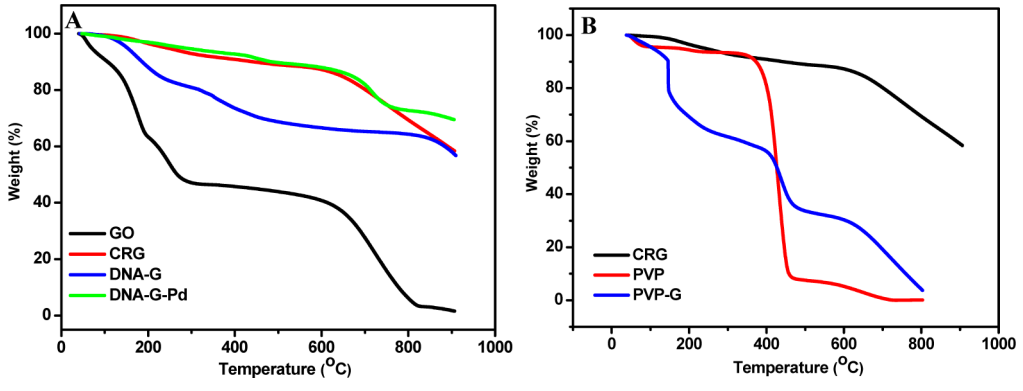

Figure 7. TGA curves of (A) GO (black), CRG (red), DNA-G (blue), and DNA-G-Pd (green); (B) CRG (black), PVP (red), and PVP-G (blue).

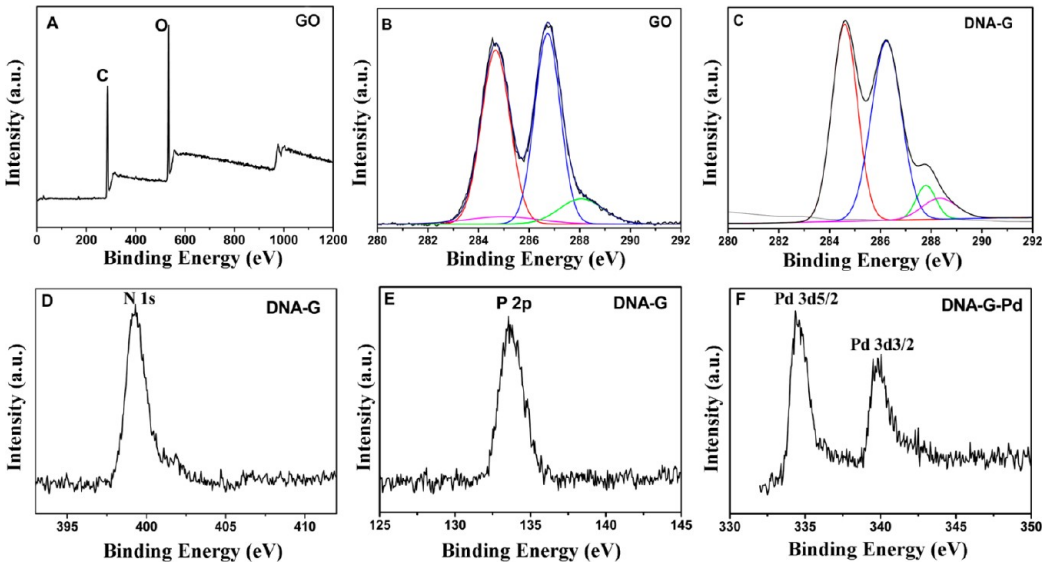

Figure 8. XPS profiles of (A) GO, (B) carbon 1s of GO, (C) carbon 1s of DNA-G, (D) nitrogen 1s of DNA-G, (E) phosphorus 2p of DNA-G, and (F) palladium 3d of DNA-G-Pd.

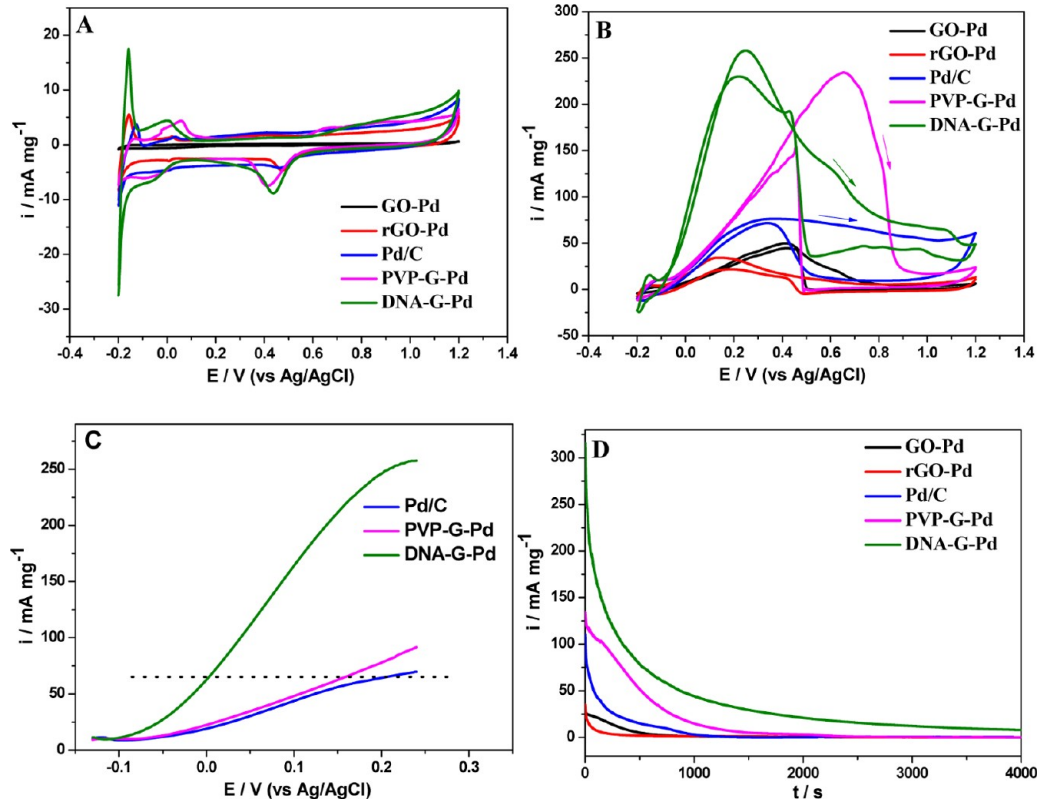

Figure 9. (A) Cyclic voltammograms (CV) of different catalysts in a nitrogen saturated aqueous solution of 0.5 M H_2SO_4 at a scan rate of 20 mV s^{-1}; (B) cyclic voltammograms and (C) linear sweep voltammetry of formic acid oxidation on the catalysts in 0.5 M H_2SO_4 + 0.5 M HCOOH solution at a scan rate of 50 mV s^{-1}; (D) chronoamperometry curves of different catalysts in 0.5 M H_2SO_4 + 0.5 M HCOOH solution at 0.25 V.

functionalities.[35] Nitrogen 1s and phosphorus 2p XPS data also confirmed that the DNA molecules were adsorbed onto the graphene sheets. These spectra showed single peaks at binding energies of 400 eV (amide, amine, and aromatic nitrogen) and 133.6 eV (P−O), respectively. XPS spectra of DNA-G-Pd clearly indicated the presence of the composition of palladium. More importantly, metallic Pd (0) is present with peaks at 335.1 and 340.0 eV (Figure 8F), indicating that palladium(II) has been reduced to Pd nanoparticles.[28,29] The slight shoulder peaks at 342.6 and 337.2 eV may be attributed to PdO due to slight oxidation of Pd NPs upon exposure to the air.

Electrocatalytic Test of Graphene/Pd Hybrid Catalysts. To assess their formic acid electro-oxidation catalytic activity, our four as-prepared materials were loaded (with the same mass loading) onto glassy carbon electrodes and measured by commonly used cyclic voltammetry (CV). Figure

9A shows the CVs of different Pd catalyst-coated electrodes in a nitrogen saturated aqueous solution of 0.5 M H_2SO_4 at a scan rate of 20 mV s^{-1}. The large region between −0.2 and −0.05 V is related to the hydrogen adsorption/desorption process on the Pd nanoparticle surface.[29,54] In addition, the reduction peak for palladium oxide is commonly observed at ca. 0.45 V (vs Ag/AgCl). According to the Coulombic amount (Q_H) associated with the peak area, the electrochemical active surface areas (ECSAs) of catalysts can be calculated using the following equation.[29]

$$\mathrm{ECSAs} = \frac{Q_H}{m \cdot C}$$

where C denotes the quantity of electricity when hydrogen molecules are adsorbed on palladium with a homogeneous and single layer (here, it is 212 μC cm^{-2}) and m is the mass of palladium on the graphene surface.

The ECSAs for DNA-G-Pd, PVP-G-Pd, Pd/C, rGO-Pd, and GO-Pd catalysts were estimated to be 82.2, 54.3, 44.5, 22.5, and 1.38 cm^2 mg^{-1}, respectively. The largest ECSAs of the DNA-G-Pd catalyst is most likely due to the smallest size and best dispersibility of Pd nanoparticles on the DNA-templated graphene among all catalysts; therefore, DNA-G-Pd catalyst could offer the most Pd active sites in the process of formic acid electro-oxidation.

Figure 9B shows the typical CVs of different catalyst-coated electrodes in 0.5 M HCOOH and 0.5 M H_2SO_4 solution at a scan rate of 50 mV s^{-1}. According to the CVs of GO-Pd and rGO-Pd, both of them show very low anodic peak current due to their poor conductance and dispersibility, respectively. For DNA-G-Pd catalyst, the main oxidation peak potential of HCOOH is located at 0.25 V, that is 0.05 V more negative than that of Pd/C catalyst (0.3 V). For PVP-G-Pd catalyst, the main oxidation peak potential is much more positive and shifts to 0.65 V, which is similar to Pt as the catalyst in HCOOH electro-oxidation,[5,6] indicating that HCOOH electro-oxidation is strongly influenced by the size, morphology, and dispersibility of Pd NPs and the properties of PVP.[55−57] In the positive-going potential scan, the mass-normalized peak current at 0.25 V on DNA-G-Pd is 228.1 mA mg^{-1}, which is 2.5-fold higher than PVP-G-Pd (92.2 mA mg^{-1}) and ∼3.5-fold better than Pd/C (64.8 mA mg^{-1}) under the same experimental conditions. Simultaneously, at any oxidation current as indicated in Figure 9C, the corresponding oxidation potentials of HCOOH on the DNA-G-Pd catalyst are obviously lower than commercial Pd/C and PVP-G-Pd. These results indicate that the DNA-G-Pd hybrid materials have superior catalytic activity for HCOOH electro-oxidation.

For evaluation of the long-term activity and durability of the prepared catalysts, chronoamperometric measurements were carried out using different catalysts at 0.25 V in 0.5 M H_2SO_4 containing 0.5 M HCOOH and the results were shown in Figure 9D. The initial current (taken at 20 s to avoid the contribution of the double-layer discharge and hydrogen adsorption) at the applied potential was consistent with the voltammograms in Figure 9B. After 1000 s, the current for Pd/C catalyst decreased to a minimum, about 2% of the initial value (Figure 9D). However, for PVP-G-Pd and DNA-G-Pd catalysts, the currents still kept 11% and 15% of the initial, respectively. After 2500 s, the current reached a constant at 0.85 mA mg^{-1} for PVP-G-Pd catalyst, whereas the current for DNA-G-Pd catalyst was 15.8 mA mg^{-1}, roughly 18.6-fold higher than that of PVP-G-Pd catalyst. As long as 4000 s, the current still remained at 8.0 mA mg^{-1} for DNA-G-Pd catalyst.

All these results demonstrate that the as-prepared DNA-G-Pd catalyst exhibits significantly higher electrocatalytic activity and durability for HCOOH electro-oxidation than the commercial Pd/C and PVP-G-Pd catalysts. This indicates that natural DNA as the mediator is playing an essential role for the hybrid catalyst. First, DNA chains provide abundant heterogeneous nucleation and anchor sites, that would facilitate the formation of the uniform and monodispersive Pd NPs in well-defined binding sites along DNA lattice. This will bring out highly electrochemical active sites on the electrode surface; these are important for electrochemical oxidation toward formic acid. Second, DNA can interact strongly with graphene sheets through $\pi-\pi$ stacking and can also chelate Pd via dative bonding, so the DNA molecule, like a glue, can enhance the hybrid material stability; moreover, the negatively charged phosphate groups on the DNA backbone can endow the three-component systems with excellent dispersibility. Third, it is known that nucleobases of DNA, such as guanine and adenine, can have irreversible, electrochemically induced oxidative damage under the applied voltage range from −0.2 to 1.2 V, further reaction would deplete oxygen in HCOOH electro-oxidation solution;[58,59] depletion of solution oxygen would restrain the conversion of Pd to PdO and decrease the deactivation of the electrochemical active surfaces of Pd and then enhance the efficiency of the electrochemical catalysis. Finally, on Pd catalyst, formic acid would follow a different oxidation reaction pathway from that on Pt catalyst. On the basis of the reaction path (eqs 1−3), both the phosphate groups and nucleobases of DNA may combine with H^+ which can greatly promote the oxidation of a formic acid reactive intermediate.[60]

$$\mathrm{HCOOH} \rightarrow \mathrm{HCOOH_{ads}} \quad (1)$$

$$\mathrm{HCOOH_{ads}} \rightarrow \mathrm{HCOO_{ads}} + \mathrm{H^+} + \mathrm{e^-} \quad (2)$$

$$\mathrm{HCOO_{ads}} \rightarrow \mathrm{CO_2} + \mathrm{H^+} + \mathrm{e^-} \quad (3)$$

More importantly, natural DNA is abundant, renewable, and biodegradable, so the DNA-G-Pd hybrid catalyst not only has high efficiency but also has low-cost and is environmentally benign.

Suzuki Reaction Catalyzed by Graphene/Pd Hybrid Catalysts. Inspired by the high activity and stability of DNA-G-Pd in formic acid electrocatalysis, the Suzuki coupling reaction was further employed as a model reaction to test the catalytic performance of DNA-G-Pd in the organic reactions.[12,61] In this reaction, phenylboronic acid is coupled with iodobenzene to give biphenyl (Scheme 1). Normally, Suzuki reactions are carried out in a mixture of an organic solvent and an aqueous inorganic base, generally under an inert atmosphere.[62] When the reaction is performed in aqueous systems under aerobic conditions, activation by phosphine ligands is generally required.[63] In this study, however, we investigated the graphene/Pd hybrid catalyzed Suzuki reaction in water containing SDS and K_3PO_4 under aerobic conditions, without any preactivation.[28]

To optimize the reaction conditions, a series of experiments with different reaction temperatures and quantities of the DNA-G-Pd catalyst was carried out. The best result in terms of yield is obtained by using 1.1 mol % DNA-G-Pd catalyst at 100 °C; the yield can reach as high as 100% in 4 min which is faster than

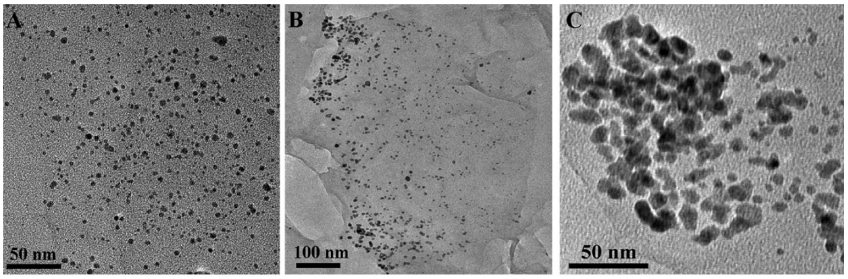

Cycle No.	1st	2nd	3rd	4th	5th	6th	7th
Conversion (%)	100	98.7	94.3	90	92.7	86.4	81.9

Figure 10. Yields in the Suzuki reaction when the DNA-G-Pd catalyst is reused at 100 °C and 4 min, and the TEM images observed after first (A), fourth (B), and seventh (C) cycles, respectively.

that which has been reported;[28] furthermore, it has no byproducts after reaction using DNA-G-Pd catalyst. (The gas chromatography (GC) results are shown in Figure S3, Supporting Information.) When carried out without SDS, the yield can also reach 95%; however, it needs 1.5 h. It has been reported that inexpensive and industrially widely used SDS has considerably extended organic chemistry in water and has a notable effect on the reaction rates.[64] When using four other prepared catalysts, the yield can reach 95.3%, 70.2%, 87.6%, and 52.7% in 4 min for PVP-G-Pd, Pd/C, GO-Pd, and rGO-Pd in the presence of SDS, respectively. This demonstrates that DNA-G-Pd has the highest activity among these five catalysts, consistent with the results of HCOOH electro-oxidation.

The DNA-G-Pd catalyst can also be reused successfully. Figure 10 shows that the DNA-G-Pd hybrid retains a reasonable performance even used in seven cycles. The yield can be as high as 80% after seven cycles. The recovery of our catalyst can be easily achieved by simple centrifugation and washing with acetone and water for several times. The morphologies of Pd nanoparticles of the recovered catalysts were examined by TEM; the typical images indicate that Pd nanoparticles are well dispersed on graphene surfaces after four cycles. Although Pd nanoparticles agglomerate to some extent after seven cycles, high conversion is kept at about 80%. It is well-known that agglomeration of Pd nanoparticles decreases the catalytic activity; hence, appropriate stabilizer or supporter is necessary to prevent deactivation by agglomeration. DNA has been reported to be an excellent template for Pd nanoparticles and nanowires.[22] DNA can provide well-defined anchor sites for Pd nanoparticles on a graphene surface, protect Pd nanoparticles from agglomeration, and keep excellent catalytic activity of Pd during the recycling process. That can be the reason why the prepared catalyst has higher catalytic activity and stability than that reported previously.[27,28]

4. CONCLUSIONS

In summary, we have developed a facile method to fabricate natural DNA-modified graphene-based Pd hybrid catalyst. The prepared DNA-G-Pd hybrid has much greater activity and durability for formic acid electro-oxidation than the commercial Pd/C catalyst and PVP-mediated graphene/Pd nanoparticle (PVP-G-Pd) hybrid used for direct formic acid fuel cells (DFAFCs). Further studies indicate that DNA-G-Pd hybrid can also be an efficient and recyclable catalyst for the organic Suzuki reaction in aqueous solution under aerobic conditions without any preactivation. To our knowledge, there is no report to show that DNA-G-Pd can be a highly active catalyst for formic acid electro-oxidation and the organic Suzuki reaction. Since DNA can chelate various transition metal cations, our work provides new insights into the design of novel catalytic materials based on graphene with full exploitation of their properties.

■ ASSOCIATED CONTENT

Ⓢ Supporting Information

Synthesis of graphene oxide (GO), XRD patterns of PVP-G and PVP-G-Pd hybrids, EDX spectra of GO, DNA-G, and DNA-G-Pd, Suzuki reaction equation, and GC results of Suzuki reaction using DNA-G-Pd as catalyst. This information is available free of charge via the Internet at http://pubs.acs.org/.

■ AUTHOR INFORMATION

Corresponding Author

*Fax: (+86) 431-85262625. E-mail: xqu@ciac.jl.cn.

Notes

The authors declare no competing financial interest.

■ ACKNOWLEDGMENTS

This work was supported by 973 Project (2011CB936004, 2012CB720602), NSFC (20831003, 90813001, 20833006, 21210002, 90913007), and Fund from the Chinese Academy of Sciences.

■ REFERENCES

(1) Winter, M.; Brodd, R. J. *Chem. Rev.* **2004**, *104*, 4245−4269.
(2) Cheng, F.; Liang, J.; Tao, Z.; Chen, J. *Adv. Mater.* **2011**, *23*, 1695−1715.
(3) Yu, X.; Pickup, P. *J. Power Sources* **2008**, *182*, 124−132.
(4) Uhm, S.; Lee, H. J.; Kwon, Y.; Lee, J. *Angew. Chem., Int. Ed.* **2008**, *47*, 10163−10166.
(5) Lee, H.; Habas, S. E.; Somorjai, G. A.; Yang, P. *J. Am. Chem. Soc.* **2008**, *130*, 5406−5407.

(6) Zhang, S.; Shao, Y.; Yin, G.; Lin, Y. *Angew. Chem., Int. Ed.* **2010**, *49*, 2211−2214.
(7) Antolini, E. *Energy Environ. Sci.* **2009**, *2*, 915−931.
(8) Mazumder, V.; Sun, S. *J. Am. Chem. Soc.* **2009**, *131*, 4588−4589.
(9) Hong, J. W.; Kim, D. H.; Lee, Y. W.; Kim, M. J.; Kang, S. W.; Han, S. W. *Angew. Chem., Int. Ed.* **2011**, *50*, 8876−8880.
(10) Wang, L.; Nemoto, Y.; Yamauchi, Y. *J. Am. Chem. Soc.* **2011**, *133*, 9674−9677.
(11) Grushin, V. V.; Alper, H. *Chem. Rev.* **1994**, *94*, 1047−1062.
(12) Astruc, D. *Inorg. Chem.* **2007**, *46*, 1884−1894.
(13) Kotha, S.; Lahiri, K.; Kishinath, D. *Tetrahedron* **2002**, *58*, 9633−9695.
(14) Polshettiwar, V.; Baruwati, B.; Varma, R. S. *Green Chem.* **2010**, *12*, 743−754.
(15) Cheong, S.; Watt, J. D.; Tilley, R. D. *Nanoscale* **2010**, *2*, 2045−2053.
(16) Novoselov, K. S.; Geim, A. K.; Morozov, S. V.; Jiang, D.; Zhang, Y.; Dubonos, S. V.; Grigorieva, I. V.; Firsov, A. A. *Science* **2004**, *306*, 666−669.
(17) Geim, A. K.; Novoselov, K. S. *Nat. Mater.* **2007**, *6*, 183−191.
(18) Stankovich, S.; Dikin, D. A.; Dommett, G. H. B.; Kohlhaas, K. M.; Zimney, E. J.; Stach, E. A.; Piner, R. D.; Nguyen, S. T.; Ruoff, R. S. *Nature* **2006**, *442*, 282−286.
(19) Zhao, C.; Feng, L.; Xu, B.; Ren, J.; Qu, X. *Chem.—Eur. J.* **2011**, *17*, 7007−7013.
(20) Gilje, S.; Han, S.; Wang, M.; Wang, K. L.; Kaner, R. B. *Nano Lett.* **2007**, *7*, 3394−3398.
(21) Song, Y. J.; Qu, K. G.; Zhao, C.; Ren, J. S.; Qu, X. *Adv. Mater.* **2010**, *22*, 2206−2210.
(22) Wang, X. H.; Wang, C. Y.; Qu, K. G.; Song, Y. J.; Ren, J. S.; Miyoshi, D.; Sugimoto, N.; Qu, X. *Adv. Funct. Mater.* **2010**, *20*, 3967−3971.
(23) Feng, L. Y.; Chen, Y.; Ren, J. S.; Qu, X. G. *Biomaterials* **2011**, *32*, 2930−2937.
(24) Hassan, H. M. A.; Abdelsayed, V.; Khder, A. E. R. S.; AbouZeid, K. M.; Terner, J.; El-Shall, M. S.; Al-Resayes, S. I.; El-Azhary, A. A. *J. Mater. Chem.* **2009**, *19*, 3832−3837.
(25) Muszynski, R.; Seger, B.; Kamat, P. V. *J. Phys. Chem. C* **2008**, *112*, 5263−5266.
(26) Zhou, X. Z.; Huang, X.; Qi, X. Y.; Wu, S. X.; Xue, C.; Boey, F. Y. C.; Yan, Q. Y.; Chen, P.; Zhang, H. *J. Phys. Chem. C* **2009**, *113*, 10842−10846.
(27) Scheuermann, G. M.; Rumi, L.; Steurer, P.; Bannwarth, W.; Mulhaupt, R. *J. Am. Chem. Soc.* **2009**, *131*, 8262−8270.
(28) Li, Y.; Fan, X.; Qi, J.; Ji, J.; Wang, S.; Zhang, G.; Zhang, F. *Nano Res.* **2010**, *3*, 429−437.
(29) Chen, X. M.; Wu, G. H.; Chen, J. M.; Chen, X.; Xie, Z. X.; Wang, X. R. *J. Am. Chem. Soc.* **2011**, *133*, 3693−3695.
(30) Yoo, E.; Okata, T.; Akita, T.; Kohyama, M.; Nakamura, J.; Honma, I. *Nano Lett.* **2009**, *9*, 2255−2259.
(31) Pileni, M. P. *Nat. Mater.* **2003**, *2*, 145−150.
(32) Fu, B. S.; Missaghi, M. N.; Downing, C. M.; Kung, M. C.; Kung, H. H.; Xiao, G. M. *Chem. Mater.* **2010**, *22*, 2181−2183.
(33) Wilson, O. M.; Scott, R. W. J.; Garcia-Martinez, J. C.; Crooks, R. M. *J. Am. Chem. Soc.* **2005**, *127*, 1015−1024.
(34) Liu, X. D.; Diao, H. Y.; Nishi, N. *Chem. Soc. Rev.* **2008**, *37*, 2745−2757.
(35) Patil, A. J.; Vickery, J. L.; Scott, T. B.; Mann, S. *Adv. Mater.* **2009**, *21*, 3159−3164.
(36) Braun, E.; Eichen, Y.; Sivan, U.; Ben-Yoseph, G. *Nature* **1998**, *391*, 775−778.
(37) Wang, Y.; Ouyang, G. H.; Zhang, J. T.; Wang, Z. Y. *Chem. Commun.* **2010**, *46*, 7912−7914.
(38) Gu, Q.; Cheng, C.; Haynie, D. T. *Nanotechnology* **2005**, *16*, 1358−1363.
(39) Kinsella, J. M.; Ivanisevic, A. *Langmuir* **2007**, *23*, 3886−3890.
(40) Dittmer, W. U.; Simmel, F. C. *Appl. Phys. Lett.* **2004**, *85*, 633−635.
(41) Mertig, M.; Ciacchi, L. C.; Seidel, R.; Pompe, W.; De Vita, A. *Nano Lett.* **2002**, *2*, 841−844.
(42) Richter, J.; Seidel, R.; Kirsch, R.; Mertig, M.; Pompe, W.; Plaschke, J.; Schackert, H. K. *Adv. Mater.* **2000**, *12*, 507−510.
(43) Nguyen, K.; Monteverde, M.; Filoramo, A.; Goux-Capes, L.; Lyonnais, S.; Jegou, P.; Viel, P.; Goffman, M.; Bourgoin, J. P. *Adv. Mater.* **2008**, *20*, 1099−1104.
(44) Hatakeyama, Y.; Umetsu, M.; Ohara, S.; Kawadai, F.; Takami, S.; Naka, T.; Adschiri, T. *Adv. Mater.* **2008**, *20*, 1122−1128.
(45) Li, X.; Peng, Y. H.; Qu, X. *Nucleic Acids Res.* **2006**, *34*, 3670−3676.
(46) Hummers, W. S.; Offeman, R. E. *J. Am. Chem. Soc.* **1958**, *80*, 1339−1339.
(47) Qu, K. G.; Ren, J. S.; Qu, X. *Mol. BioSyst.* **2011**, *7*, 2681−2687.
(48) Wei, W. L.; Qu, K. G.; Ren, J. S.; Qu, X. *Chem. Sci.* **2011**, *2*, 2050−2056.
(49) Yang, H. F.; Zhang, Q. X.; Shan, C. S.; Li, F. H.; Han, D. X.; Niu, L. *Langmuir* **2010**, *26*, 6708−6712.
(50) Stankovich, S.; Dikin, D. A.; Piner, R. D.; Kohlhaas, K. A.; Kleinhammes, A.; Jia, Y. Y.; Wu, Y.; Nguyen, S. T.; Ruoff, R. S. *Carbon* **2007**, *45*, 1558−1565.
(51) Tuinstra, F.; Koenig, J. L. *J. Chem. Phys.* **1970**, *53*, 1126−1130.
(52) Jasuja, K.; Berry, V. *ACS Nano* **2009**, *3*, 2358−2366.
(53) Lin, Y.; Watson, K. A.; Fallbach, M. J.; Ghose, S.; Smith, J. G.; Delozier, D. M.; Cao, W.; Crooks, R. E.; Connell, J. W. *ACS Nano* **2009**, *3*, 871−884.
(54) Zhang, J. T.; Qiu, C. C.; Ma, H. Y.; Liu, X. Y. *J. Phys. Chem. C* **2008**, *112*, 13970−13975.
(55) Chen, Y. X.; Heinen, M.; Jusys, Z.; Behm, R. J. *Angew. Chem., Int. Ed.* **2006**, *45*, 981−985.
(56) Hoshi, N.; Kida, K.; Nakamura, M.; Nakada, M.; Osada, K. *J. Phys. Chem. B* **2006**, *110*, 12480−12484.
(57) Zhou, W.; Lee, J. *J. Phys. Chem. C* **2008**, *112*, 3789−3793.
(58) Yang, I. V.; Throp, H. H. *Inorg. Chem.* **2000**, *39*, 4969−4976.
(59) Napier, M. E.; Hull, D. O.; Throp, H. H. *J. Am. Chem. Soc.* **2005**, *127*, 11952−11953.
(60) Yang, S. D.; Zhang, X. G.; Mi, H. Y.; Ye, X. G. *J. Power Sources* **2008**, *175*, 26−32.
(61) Wang, F.; Li, C. H.; Sun, L. D.; Wu, H. S.; Ming, T.; Wang, J. F.; Yu, J. C.; Yan, C. H. *J. Am. Chem. Soc.* **2011**, *133*, 1106−1111.
(62) Littke, A. F.; Dai, C. Y.; Fu, G. C. *J. Am. Chem. Soc.* **2000**, *122*, 4020−4028.
(63) Goossen, L. J.; Ghosh, K. *Angew. Chem., Int. Ed.* **2001**, *40*, 3458−3460.
(64) Xin, B. W.; Zhang, Y. H.; Cheng, K. *Synthesis* **2007**, *13*, 1970−1978.